SUPPLEMENTARY INFORMATION

Non-volatile ionic modification of the Dzyaloshinskii Moriya Interaction

L. Herrera Diez,[1,*] Y.T. Liu,[1,*] D. A. Gilbert,[2,3] M. Belmeguenai,[4] J. Vogel,[5] S. Pizzini,[5] E. Martinez,[6] A. Lamperti,[7] J. B. Mohammedi,[8] A. Laborieux,[1] Y. Roussigné,[4] A. J. Grutter,[2] E. Arenholtz,[9] P. Quarterman,[2] B. Maranville,[2] S. Ono,[10] M. Salah El Hadri,[11] R. Tolley,[11] E. Fullerton,[11] L. Sanchez-Tejerina,[12] A. Stashkevich,[4] S. M. Chérif,[4] A. D. Kent,[8] D. Querlioz,[1] J. Langer,[13] B. Ocker,[13] and D. Ravelosona[1]

[1]*Centre de Nanosciences et de Nanotechnologies, CNRS, Univ. Paris-Sud, Université Paris-Saclay, C2N Palaiseau, 91120 Orsay cedex, France*[†]

[2]*NIST Center for Neutron Research, National Institute of Standards and Technology, Gaithersburg, Maryland 20899, USA.*

[3]*Department of Materials Science and Engineering, University of Tennessee, Knoxville, Tennessee 37919, USA.*

[4]*Laboratoire des Sciences des Procédés et des Matériaux, CNRS-UPR 3407, Université Paris 13, Sorbonne Paris Cité, 93430 Villetaneuse, France.*

[5]*Univ. Grenoble Alpes, CNRS, Institut Néel, 38000 Grenoble, France.*

[6]*Departamento de Física Aplicada, Universidad de Salamanca, Plaza de la Merced s/n. 37008 Salamanca, Spain*

[7]*IMM-CNR, Unit of Agrate Brianza,, Via C. Olivetti 2, 20864 Agrate Brianza (MB), Italy.*

[8]*Department of Physics, New York University, New York, New York 10003, USA.*

[9]*Advanced Light Source, Lawrence Berkeley National Laboratory, Berkeley, California 94720, USA.*

[10]*Central Research Institute of Electric Power Industry, Yokosuka,Kanagawa 240-0196, Japan.*

[11]*Center for Memory and Recording Research,*
University of California, San Diego,
La Jolla, California 92093-0401, USA
[12]*Dpto. Electricidad y Electronica,*
University of Valladolid, 47011 Valladolid, Spain
[13]*Singulus Technology AG, Hanauer Landstrasse 103, 63796 Kahl am Main, Germany.*

*These authors contributed equally to this work

†Electronic address: liza.herrera-diez@c2n.upsaclay.fr

Sample growth and device structure

The magnetic materials used in this study are Si/SiO_2/Pt (3 nm)/Co (0.6 nm)/HfO_2 (3 nm) films grown by magnetron sputtering. To incorporate the gate to the device, the IL [EMI][TFSI] (1-ethyl-3 methylimidazolium bis(trifluoromethanesulfonyl)imide) is added to the surface of the film. A counter electrode, a glass substrate coated with indium tin oxide (ITO) is then placed on top of the IL. The counter electrode and the magnetic sample have been connected by using Ag paste and wires. The size of the E-field biased Co area varies between 0.25 cm^2 and 1 cm^2. In all cases, after the application of the E-field, the top electrode was removed and the IL wiped off to conduct measurements on the bare films after the permanent E-field induced property modulations. The HfO_2 layers were deposited in situ by magnetron sputtering from an HfO_2 target. Samples were always stored in air and at room temperature before conducting the gating experiments.

The value of the E-field that is applied by the liquid gate is calculated by dividing the applied voltage by a distance of 5 nm, which accounts for the 3 nm of HfO_2 and for an effective 2 nm separation due to the presence of the IL. This last estimation is done taking into account only the distance over which an electric double layer is formed at the side of each one of the electrodes (1 nm) [18] and not the total thickness of the liquid layer.

XAS and XPS

XAS measurements were performed on BL 4.0.2 at the Advanced Light Source by sweeping the X-ray energy through the Co-$L_{2,3}$, Hf-M_5, and O-K resonant edges. Measurements were performed in total-electron yield mode with the X-rays applied in the plane of the film. XPS measurements were taken using a PHI ESCA 5600 apparatus equipped with a monochromatic Al Kα X-ray source (energy = 1486.6 eV) and a concentric hemispherical analyzer. The spectra were collected at a take-off angle of 45° and a band-pass energy of 58.70 eV. The spectra were aligned using the C 1s peak (284.6 eV) from adventitious carbon as reference.

PNR and SLD

PNR measurements were performed at the NIST Center for Neutron Research using the MAGIK reflectometer. Measurements were performed at room-temperature, using 5Å neutrons, and with a saturating magnetic field of 600 mT applied in the plane of the film which was reduced to 200 mT during the measurement. The model was fit to the data using the Refl1D [46] software package. All of the models converged to $\chi^2 < 3$.

As mentioned in the main text, a broadening of the SiO_2/Pt interface, and an increase in the Pt thickness is observed. One alternative explanation of this observation could be the injection of OH^- ions into the Pt and accumulation at the Pt interfaces. Specifically, the injection of OH^- ions would swell the Pt lattice, increasing the apparent thickness. Calculating the nuclear SLD, the OH^- ions possess a combined nuclear scattering length of 2.1 fm, compared to Pt at 9.6 fm or O^{-2} at 5.8 fm, thus as the film gets slightly thicker, and these weaker scattering centers are incorporated, the overall SLD changes very little. The nuclear SLD of the Co layer initially appears larger than the bulk value (2.26 x10^{-6} $Å^{-2}$) and decreases with increased E-field biasing time. The large initial SLD is partly an artifact due to overlapping of the interfaces, but also could suggest a partial oxidation of the as-grown (AG) film, while a decrease can be achieved by the injection of an element with negative scattering length, which in this system could only be hydrogen, the removal of a positive SLD element or a decrease in the atomic density. While a lattice expansion can be achieved by oxygen or OH^- injection, this would increase the nuclear SLD contrary to what is observed here, this is the reason that a proposed mechanism involving binding and recombination of the inserted OH^- groups is proposed.

Reversibility measurements

Figure S1 presents Hall effect measurements of a sample that is initially in the AG state (black symbols) and is subsequently biased for 1 min under a +3V gate voltage (red symbols). The sample does not show an effect in the magnetic response while when the same sample is subsequently biased for 1 min at a gate voltage of -3V a square hysteresis loop is obtained indicating a spin reorientation transition (blue symbols). A positive gate voltage has no effect either on the magnetic properties of the AG sample or on its potential

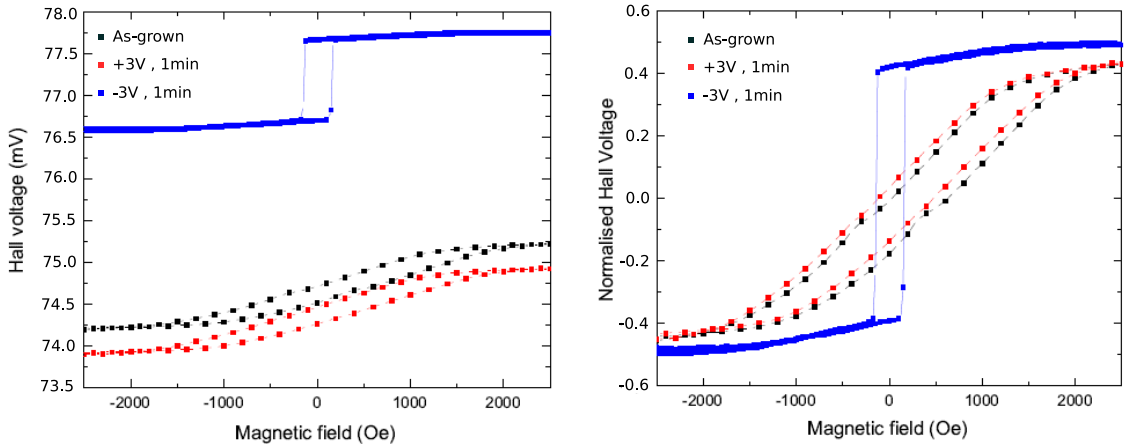

FIG. S1: Effects of positive and negative gate voltages on an AG sample. Only the negative voltage shows a significant effect.

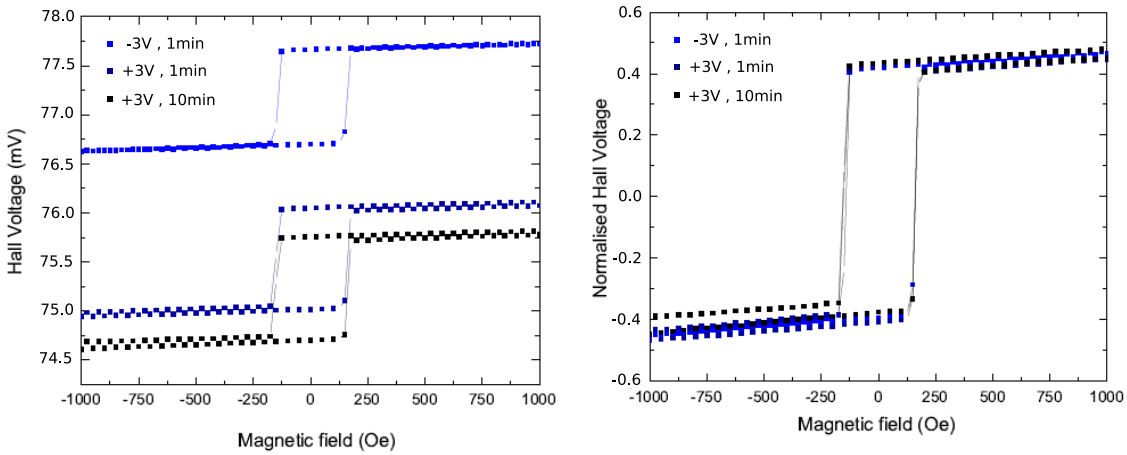

FIG. S2: No effects are observed by applying a +3V gate voltage on a previously negatively biased sample (light blue) for either 1 min (dark blue) or 10 min (black).

to undergo a spin reorientation transition under the subsequent exposure to a negative gate voltage. The normalised curves are shown on the right hand side panel.

The non-reversibility of the magnetic state achieved by the application of -3V for 1 min (light blue symbols) is shown in Fig. S2. A gate voltage of +3V is applied to this sample for 1 min (dark blue symbols) and subsequently for 10 min (black symbols) without obtaining any changes in the magnetic response. The right hand panel shows the normalised curves. Positive voltages well outside of the electrochemical window of the IL have also been applied and are shown in Fig. S3. Even in this unreliable and highly reactive regime, no effects

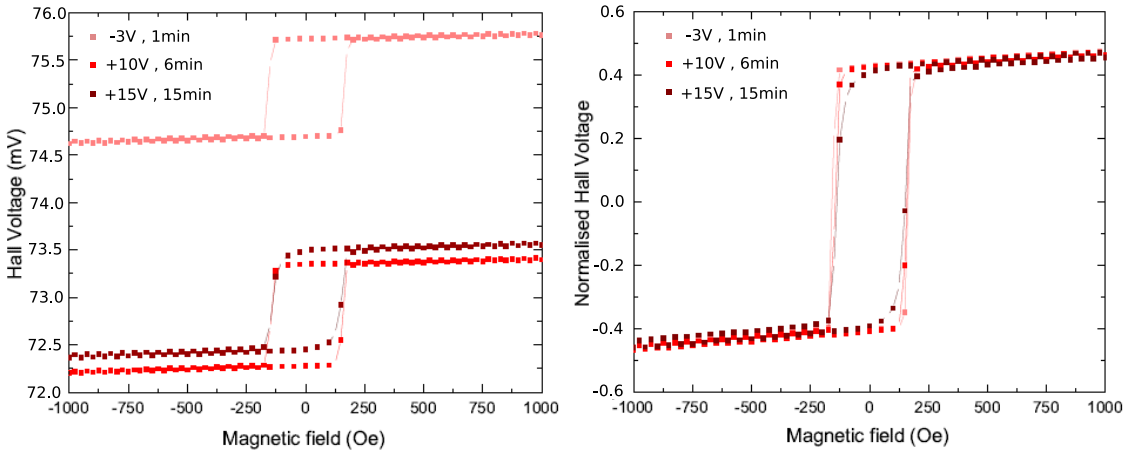

FIG. S3: No significant effects are observed even when applying gate voltages well outside of the electrochemical window, +10V (red) and +15V (dark red), to a previously negatively biased sample (light red).

were observed in the magnetic response of the previously negatively biased film (light red) under +10V for 6min (red), only a very small variation in the squareness of the loop is seen after a subsequent +15V gate voltage exposure for 15min (dark red).

Reversibility has also been tested for smaller effects induced by a negative gate voltage. Fig.S4 shows an AG sample before (black) and after (red) applying a gate voltage of +3V for 10 min, which does not induce any significant changes. Subsequently a voltage ramp to -3V is performed (or a duration of about 50s, as in every other experiments) and once reaching -3V the voltage is removed immediately. After this procedure the sample shows to have a more significant alignment with the perpendicular direction (blue) without being fully in the PMA state. This sample was subsequently exposed to a gate voltage of +3V for 6min (dark blue). The magnetic response seems to move towards the initial state (weaker PMA), however the effects are very small.

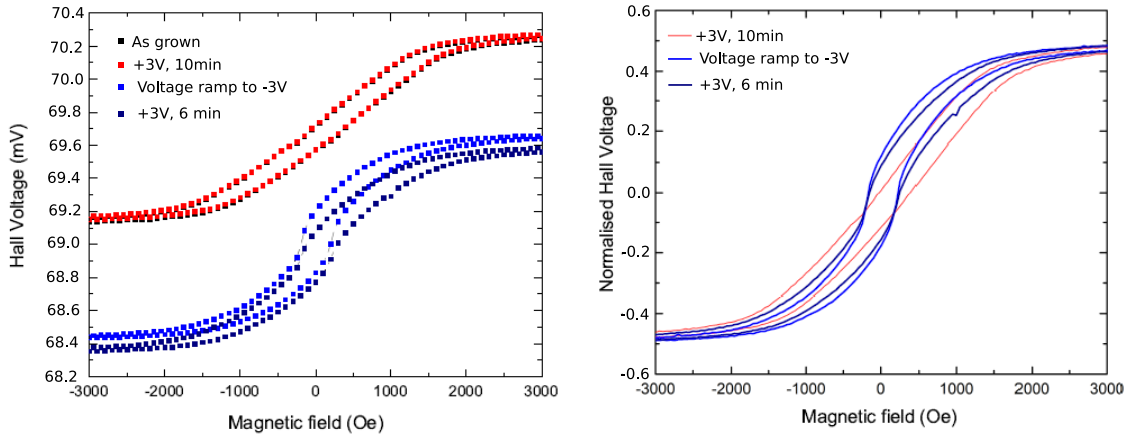

FIG. S4: An AG sample (black) is initially exposed to +3V for 10 min (red). Subsequently, the sample is exposed only to a gate voltage ramp to -3V (blue) and to a +3V gate voltage for 6 min (dark blue). A very small recovery of the initial magnetic properties is observed.

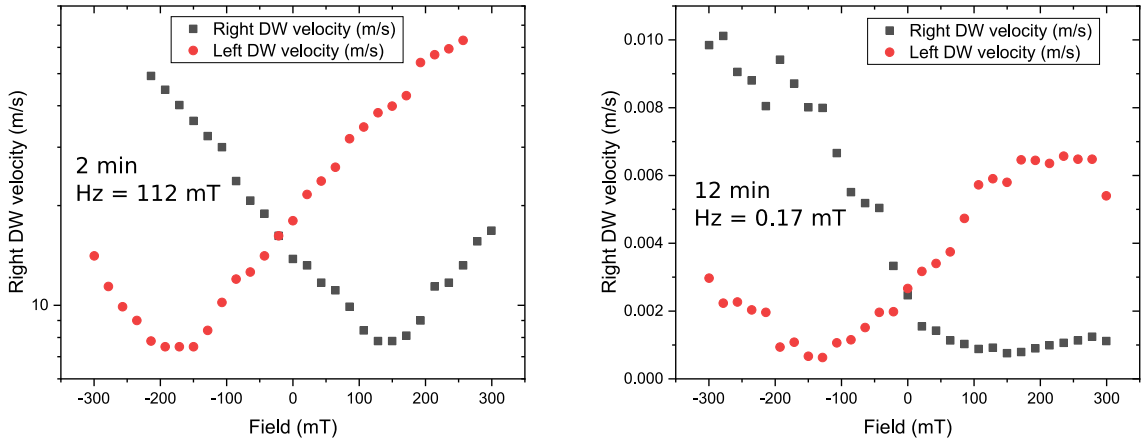

FIG. S5: Domain wall velocity curves under an in-plane field for samples biased for 2min and 12min. The minima indicate the DMI field that allows to extract the value of D.

Domain wall motion experiments

The additional domain wall velocity curves as a function of an in-plane magnetic field used to determine the value of DMI that complete the full data set presented in the main text are shown in Fig.S5. The out of plane fields used for the 2 min and 12 min samples are 112 mT and 0.17 mT, respectively. The high nucleation rate in the 12 min sample did not allow us to conduct velocity measurements outside of the creep regime.

Domain wall motion experiments under only a perpendicular field have also been conducted

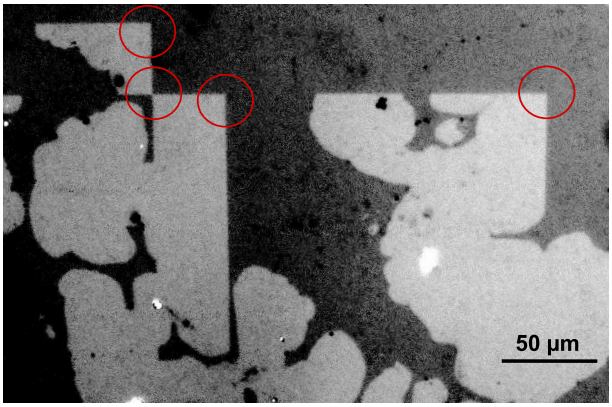

FIG. S6: Domain expansion in a film exposed to the E-field for 22 minutes. The red circles mark the 90° crossing of E-field induced pinning lines.

in samples biased for 22 minutes, where a clear ferromagnetic order is still present in the Co layer (see Fig.S6). However, a large number of structural defects can be observed in the domain pattern. Interestingly, the defects in the films biased for 22 minutes can be found to be extremely regular in some parts, as shown in Fig.S6, where pinning lines can be found to cross at 90°. This could be compatible with a strain related effect at the interface with the SiO_2 substrate due to ionic anchoring, as discussed in the main text.

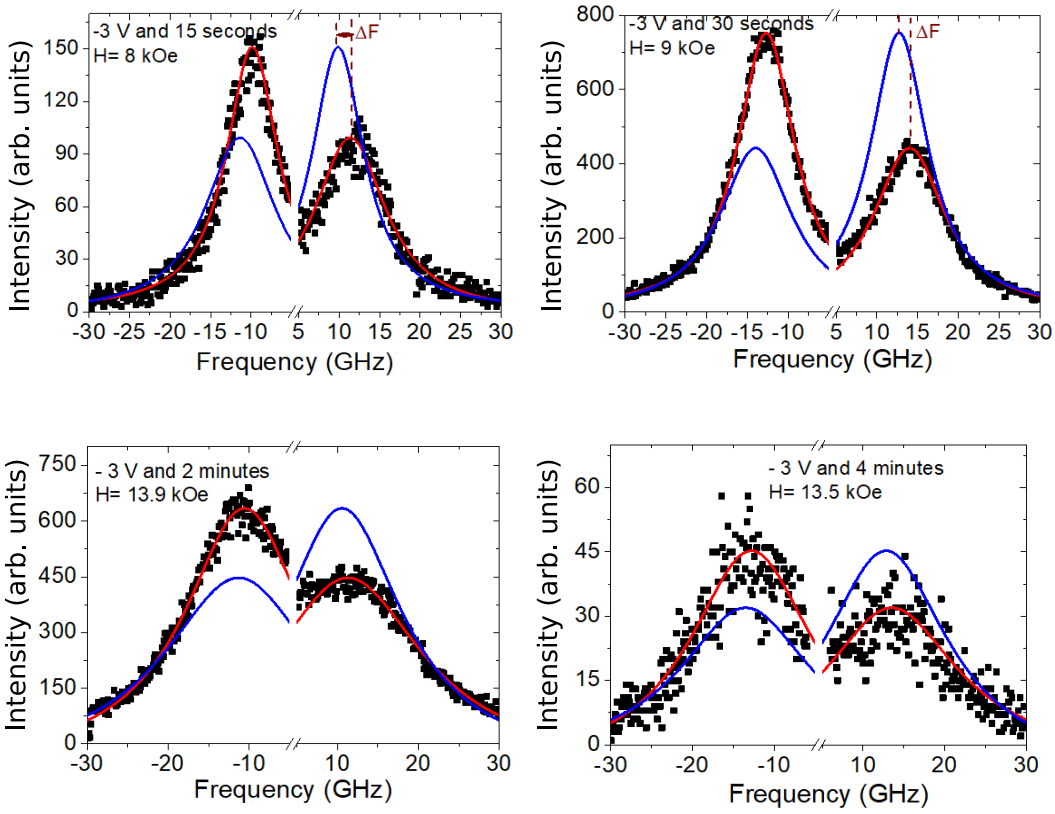

FIG. S7: BLS spectra and Lorentzian fitting for samples biased for 15s, 30s, 2 min and 4 min. The asymmetry between the peaks reduces for high biasing times.

Brillouin light scattering spectroscopy (BLS)

BLS in Damon-Eshbach geometry has been used to record the spin wave spectra, after counting photons up to 12 hours, as a function of the in-plane applied magnetic field and for various wave vector values. The sample was illuminated with a laser with wavelength λ = 532 nm.

The additional BLS spectra that complete the full data set presented in the main text are shown in Fig.S7. The linewidth is seen to increase with biasing time that could be linked to an increasing inhomogeneity of magnetic anisotropy and/or an increase in the damping parameter α at high biasing times.

Micromagnetic simulations

The value of the Gilbert damping parameter α has been chosen to be 0.5 for the 1 minute sample, a value consistent with those found in the literature for Pt/Co films [25], while it has been fixed to 0.8 and 1 for the samples biased for 2 minutes and 4 minutes, respectively. For longer biasing times we have increased the value of α based on the structural changes observed. We have concluded that in this regime a significant E-field induced disorder at the Pt/Co interface could lead to a higher degree of alloying of Co with a high spin orbit coupling material (Pt) which can certainly lead to an increase in damping.

When all experimental values of K_{eff}, M_s, D (DW motion values) and A (including an extrapolation for the sample biased for 2 minutes) are introduced in the simulations a good correspondence between the simulations and the experimental DW velocity curves is obtained only in the lower field region, appearing before the velocity plateaux, which is more sensitive to the values of α as will be shown later. However, the velocity plateaux can not be reproduced using the experimental D values obtained either by BLS or by DW motion and are weakly dependent on α as reported in the literature [**?**]. A higher value of D lifts the plateaux to higher velocity values for all curves and allows for a better correspondence with the experimental data confirming the high sensitivity of the velocity plateau to the value of D and that the E-field induced decrease observed can be directly linked to the reported reduction in D.

As mentioned in the main text, a distribution of 20% in the parameters M_s, K_u (the uniaxial anisotropy constant), u_K (the direction of the easy axis) and D with respect to the experimentally determined values was introduced for the calculations shown in the left side panel of Fig.S8. In the right side panel only M_s, K_u and u_K are allowed to show a distribution of values. For these two cases the Gilbert damping parameter α has been fixed to 0.5. It can be observed that the two set of curves do not change significantly upon the introduction of a distribution in the D values, only a small increase in the DW velocity plateau appearing in the range ≈150-250 mT is observed upon fixing the value of D. Most importantly the profile of the velocity curves at high fields is far smaller than the values observed experimentally in both cases.

The effects of varying the Gilbert damping parameter α are presented in Fig. S9. As mentioned earlier, the values of α seem to predominantly have an impact on the velocity

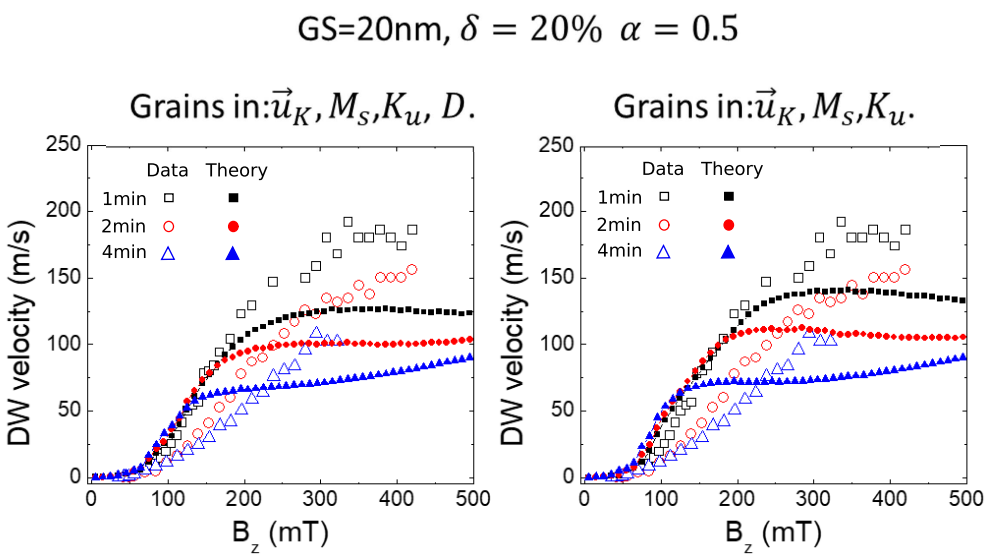

FIG. S8: Mumax simulations showing the effects of allowing a distribution of D values. No significant changes are observed by introducing a distribution in the value of D.

curves between the exponential regime and the velocity plateau while the maximum velocity does not seem to be greatly influenced. The values that give the best correspondence with the experimental data (excluding the high field velocity plateau) seem to have the tendency to increase with the E-field bias time. This is in agreement with the BLS spectra which show a broadening of the peaks as the E-field bias time increases. This broadening can be related to an increase in α but it can also contain a component related to the increase in inhomogeneity of the sample's properties. A more detail analysis of both effects is required to be able to extract quantitative information on α from the BLS data.

Finally, as the velocity plateau does not seem to be greatly influenced by including a distribution of D values nor by the value of α, D was allowed to change in order to evaluate the existence of a better correspondence between the experimental and simulated velocity curves. As presented in the main text, a good correspondence is achieved by using higher values of D that those obtained experimentally.

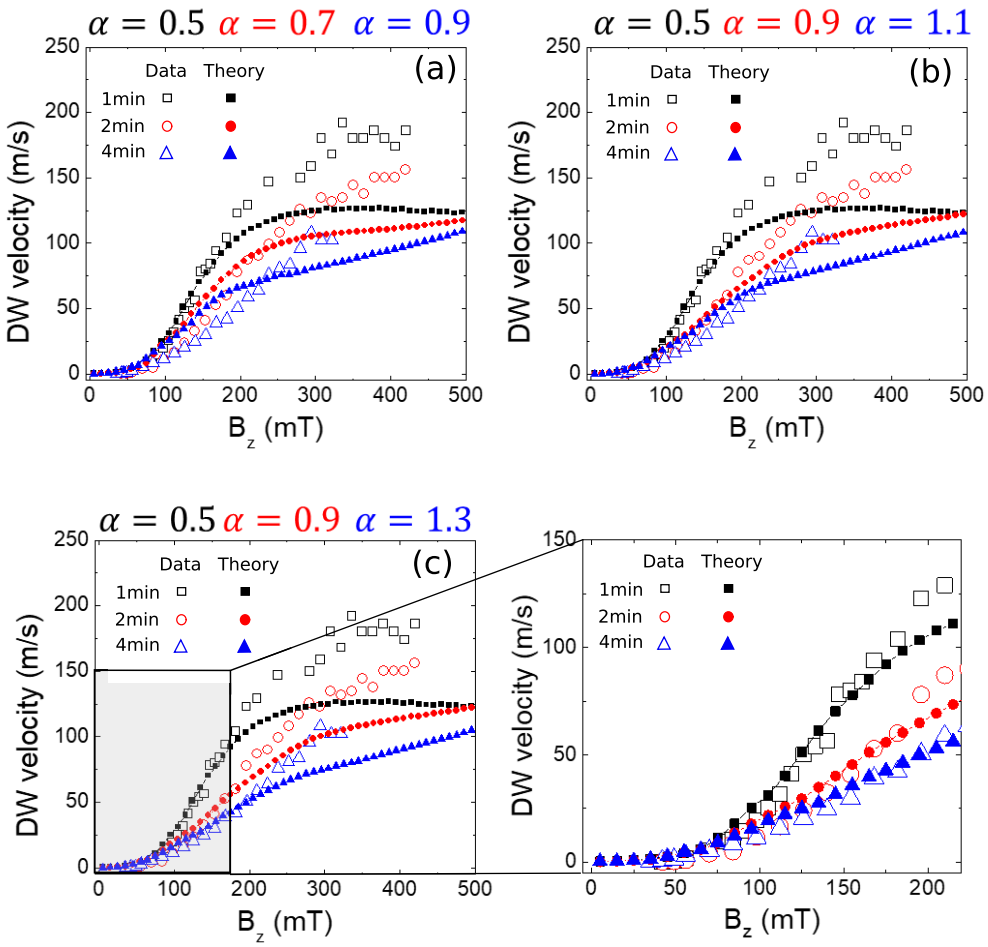

FIG. S9: Mumax simulations showing the effects of changing the value of the Gilbert damping parameter α for the three data sets corresponding to the samples biased for 1 min, 2 min and 4 min.

X-Ray Photoelectron Spectroscopy

Figure S10 shows the Hf $4f$ and O $1s$ XPS peaks for the as grown and 4 min biased samples that complete the dataset presented in the main article. There is no significant effect of the electric field.

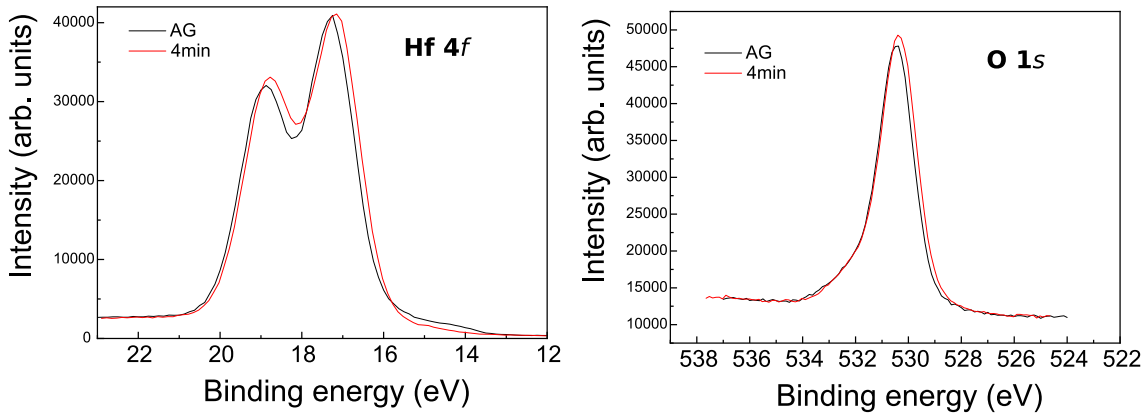

FIG. S10: Hf $4f$ and O $1s$ XPS peaks for the as grown and 4 min biased samples. No significant changes are observed upon E-field application.

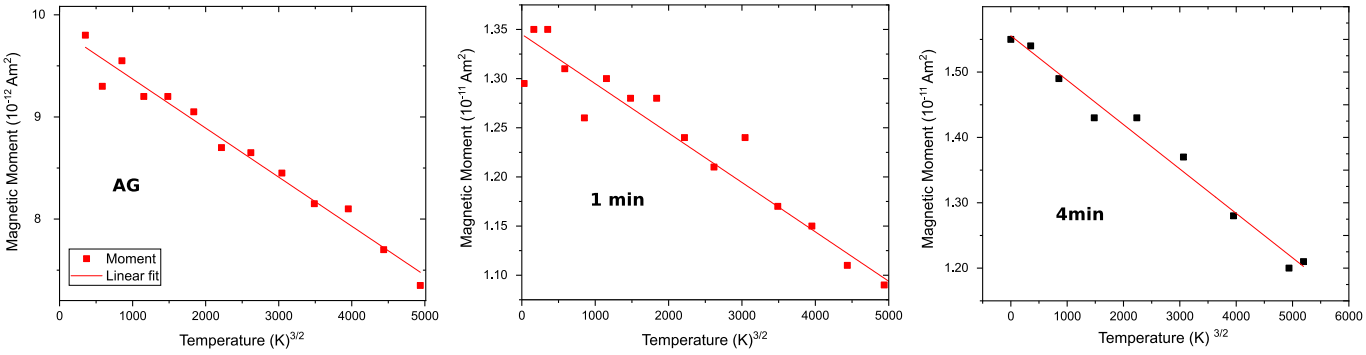

FIG. S11: Magnetic moment dependence on $T^{3/2}$ for the AG sample and those biased for 1 min and 4 min. The linear fits used to extract A are shown as solid lines.

Extraction of the exchange stiffness constant A

The extraction of the value of A is based on [23], which uses the Bloch-$T^{3/2}$ law describing the magnetization decrease associated with thermally excited magnons to analyse the temperature dependence of the magnetic moment. The curve of magnetic moment vs. $T^{3/2}$ for the AG sample and those biased for 1min and 4 min are presented in Fig. S11. The data is plotted together with their corresponding linear fitting lines. The prefactor η needed to calculate A using the Bloch law has been approximated to 0.7 by extrapolating the values calculated in [23] for a 0.6 nm thick film.

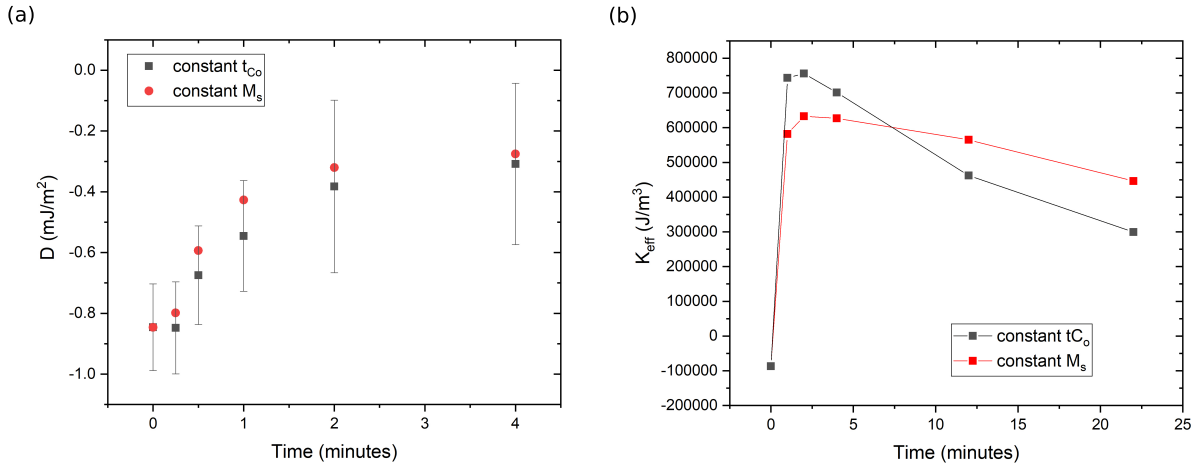

FIG. S12: D (a) and K_{eff} (b) values calculated using a constant M_s (red) or a constant t_{Co} (black) as in the main text. Small variations in the values are observed in the case of a thickness modulation and the trends are conserved in both cases.

Considerations on a potential E-field induced variation of the thickness of the Co films

In this section we want to discuss the potential impact of a variation in the thickness of the Co layer (t_{Co}) induced by the E-field in the calculated parameters.

The values of D extracted from BLS depend on the value of t_{Co} through their dependence on M_s. In order to analise a potential variation in t_{Co} caused by the E-field treatment we have calculated D using a constant M_s value corresponding to the pristine film for all samples. By doing this we are evaluating the results of the extreme scenario where the full measured variation in the magnetic moment is only due to a change in thickness and not to a variation of M_s. If we compare these values to the calculation presented in the main text (using the measured values of M_s considering a constant t_{Co}) the differences in the value of D between the two methods are within the error bar, which assures the validity of our results beyond a potential variation in t_{Co}. This comparison is shown in Fig.S12 (a).

A potential t_{Co} variation could also impact the extraction of the value of K_{eff}. However, as in the case of the D values obtained by BLS we have calculated the values of K_{eff} using both a constant t_{Co} and a constant M_s, as shown in Fig.S12 (b). The values present the largest variations in the order of 25%, however, the trend is conserved.

A potential variation could also be expected for the values of A since they are based on the temperature variation of M_s, however, for this we also expect a similar variation as the one calculated for K_{eff} and D. In addition, a potential variation of t_{Co} should affect more the intercept of the M_s vs. T curve than the slope, which is the parameter used to extract A, minimising a potential variation.

It is worth noting that the extraction of the D values by BLS does not depend on the accuracy of the measured values of K_{eff} or A, which is the case for the values derived by domain wall motion. This could be a source of discrepancy between the two data sets as mentioned in the main text.